Mechanical Systems and Signal Processing 149 (2021) 107179

Contents lists available at ScienceDirect

Mechanical Systems and Signal Processing

journal homepage: www.elsevier.com/locate/ymssp

Locally resonant metamaterial curved double wall to improve sound insulation at the ring frequency and mass-spring-mass resonance

Zibo Liu [a], Romain Rumpler [a,b,*], Leping Feng [a]

[a] The Marcus Wallenberg Laboratory for Sound and Vibration Research (MWL), Department of Engineering Mechanics, KTH Royal Institute of Technology, SE-100 44 Stockholm, Sweden
[b] Centre for ECO2 Vehicle Design, KTH Royal Institute of Technology, SE-100 44 Stockholm, Sweden

ARTICLE INFO

Article history:
Received 12 February 2020
Received in revised form 20 July 2020
Accepted 29 July 2020
Available online 14 August 2020

Keywords:
Locally resonant metamaterial
Curved double wall
Ring frequency
Mass-spring-mass resonance
Impedance approach
Sound transmission loss

ABSTRACT

A locally resonant metamaterial curved double wall is proposed and studied. The aim is to improve the sound insulation by introducing a metamaterial design targeting a narrow frequency band region associated with characteristic frequencies of curved double walls, thus enabling an overall improvement of sound insulation properties in a broader frequency range. This metamaterial is realized by introducing periodically distributed resonators to a curved double wall. The sound transmission loss properties of such curved double walls are first investigated by using the concept of 'apparent impedance', which expresses the properties of the whole structure in terms of the impedances of the constituting panels and air cavity. The apparent impedance approach is validated against Finite Element models. It is shown that, instead of a dip in the sound transmission loss around the ring frequency of a single curved panel, the curved double wall may exhibit a broad 'valley' with low sound transmission loss, whose bandwidth is determined by the spacing between the two characteristic frequencies of the structure (associated with the ring frequency and mass-spring-mass resonance of the curved double wall). The curved double wall is then specifically designed by adjusting the two characteristic frequencies to be close to each other in order to narrow the region associated with a low transmission loss. This enables, subsequently, to improve the transmission loss in this region by effectively inserting tuned local resonators. The design principles are discussed, and applications of double walls consisting either of the same curved panels or different curved panels are both included.

1. Introduction

Curved double walls or similar structures are among the commonly used structures in the transport industry, such as in the aerospace industry. However, the combination of curved panels, and a double wall arrangement may exhibit reduced acoustic insulation properties at specific frequencies. For curved acoustic panels, the ring frequency is one of the frequencies where low acoustic insulation performance occurs. Double-wall structures, on the other hand, may be strongly affected due to the mass-spring-mass resonance effect, which may result in a low sound transmission loss. Extensive research has been conducted in order to improve the acoustic properties of curved panels alone [1–12] or double walls [13–20]. However, the

* Corresponding author.
E-mail addresses: zibo@kth.se (Z. Liu), rumpler@kth.se (R. Rumpler), fengl@kth.se (L. Feng).

https://doi.org/10.1016/j.ymssp.2020.107179
0888-3270/

sound insulation performance for curved double-wall structures may be even more critical since the sound transmission loss is not only affected by the ring frequency effect, but also by the mass-spring-mass resonance effect. Research with respect to the acoustic properties of such curved double-wall panels may be found in [21–23]. However, to the authors' knowledge, limited contributions have focused on the specific improvement of sound insulation performance of such structures around the critical frequencies mentioned above.

In recent years, numerous studies have been devoted to the development of locally resonant metamaterial acoustic panels for sound insulation purposes [12,19,24–33]. Such metamaterial panels usually consist of a host panel and periodically placed local resonators, which are specifically tuned to target frequencies with low sound insulation performance. These metamaterial acoustic panels potentially exhibit excellent sound insulation in certain frequency bands due to the presence of internal resonances. For example, locally resonant metamaterial panels have shown to be effective to overcome the coincidence effect of single-leaf panels and sandwich panels [25,26,30]. However, it has been shown, both numerically and experimentally, that the resonance only results in a narrow working frequency range and may sometimes even lead to an adverse effect, *e.g.* when tuning the resonance frequency at the ring frequency of curved panels [12,34], or at the mass-spring-mass resonance frequency of double walls [33,35]. These characteristics may be studied by the introduction of methods such as the equivalent mass/stiffness theory [25,34,35], or the stopband theory [31,36,37], which provide a measure of insight into the associated physical behaviour. In general, the sound insulation effect of the metamaterial panel is governed by the resonator at the resonance frequency, and such resonance may only occur in a very narrow frequency band, thus limiting the application potential of such metamaterial design.

On the basis of these limitations, a specific design of the curved double wall is investigated in this paper. In this design, the two characteristic frequencies (associated with the ring frequencies and the mass-spring-mass resonance effect), which lead to reductions in sound transmission loss, are tuned to be close to each other, such that their bad acoustic performance may be dealt with simultaneously. In particular, the combined effect of the ring frequencies and the mass-spring-mass resonance frequency may be addressed using localized resonators. The present paper focuses on studying the sound insulation properties of such metamaterial curved double walls, exploring the possibility to improve the sound insulation performance in the low frequency range. A more general description of curved double walls is considered in this work, as shown in Fig. 1, compared to concentric double-wall cylindrical shells, generally suitable for ducts, as may be found in [21–23]. Note that the outer panels of the double-wall structure need not be identical, given that double walls consisting of identical outer panels generally display lower sound insulation performance, due to the mass-spring-mass resonance, than those with different outer panels.

The investigation conducted is based on an impedance approach and the Finite Element method. Developed on the basis of Heckl's theory [38] and effective mass theory [34], the impedance approach implemented in this paper is used for fast estimations of the sound transmission loss of curved double-wall panels. In order to estimate the sound transmission loss of the double wall, an 'apparent impedance' is introduced, which is then extended to the case of the curved double wall and the associated metamaterial design. With this approach, the low sound insulation performance may be effectively detected by locating a minimum in the expression of the 'apparent impedance'. This minimum in the impedance in itself provides a physical explanation for the reduced sound insulation performance at such frequencies. As an alternative computational method to the equivalent mass/stiffness theory for the sound insulation prediction of metamaterial structures [25,33], the impedance approach not only provides potential insight, but also a fast and reliable tool prior to a time-consuming and computationally expensive numerical simulation. The Finite Element model used for validation is established in three dimensions for panels infinitely long in one direction and bounded in the other direction. Together with validation purposes, it also provides additional detailed results corresponding to more realistic configurations.

The paper is organized as follows: Section 2 introduces an impedance approach for the sound transmission loss estimation of a metamaterial curved double wall; in Section 3, the sound transmission loss of identical curved double walls, *i.e.* double walls made of the same curved panels, is analyzed, followed by a metamaterial design for the curved double wall deriving from this analysis; Section 4 further extends the case to nonidentical curved double walls, where the double-wall layout comprises different curved panels; the conclusions are drawn in Section 5.

2. Impedance approach

In this Section, an impedance approach is detailed in order to estimate the sound transmission loss of curved double-wall panels and their associated locally resonant metamaterial design.

The sound transmission loss estimation is based on a classical model of sound transmission through an unbounded panel. For this purpose, the panel is placed at the interface between two semi-infinite air domains and excited by time-harmonic

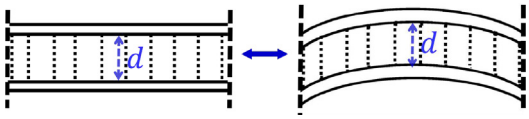

Fig. 1. A schematic view of a double wall and a curved double wall.

oblique incident acoustic plane waves, whose time-dependence is of the form $e^{j\omega t}$, where $j = \sqrt{-1}$, omitted in the rest of the paper. The panel impedance may be derived by considering the ratio of the acoustic pressure difference between the two sides of the panel to the normal component of the particle velocity.

In order to properly estimate the impedance of the panels of interest here, an 'apparent impedance' for a double wall is introduced. By further inserting the impedance associated with curved panels in this expression, the 'apparent impedance' of the curved double wall may be obtained. Based on this 'apparent impedance', the properties of the ring frequencies and the mass-spring-mass resonance of the curved double wall are then analyzed.

Further, in order to determine the effective impedance of the metamaterial, the equivalent impedance associated with the resonators is introduced into the 'apparent impedance' of the curved double wall. These steps are detailed in the subsections below.

2.1. Sound transmission loss

The sound transmission loss is given by

$$\mathrm{STL} = 10\log\left(\frac{1}{\tau}\right),$$

where τ is the transmission coefficient. With an incident angle θ with respect to the normal direction of the panel, τ may be expressed in the form of

$$\tau = \left|1 + \frac{Z}{2Z_a}\right|^{-2}, \tag{1}$$

where Z is the impedance of the panel and $Z_a = \rho_0 c_0/\cos\theta$, with ρ_0 the density of the air and c_0 the speed of sound in the air.

2.2. 'Apparent impedance' of a double wall

A double-wall system typically consists of two panels and an internal resilient material. When the internal material is assumed to be locally reacting to the acoustic excitations, (*e.g.*, when there are fibrous materials between the walls), the transmission coefficient for a flat double-wall system may be given, as detailed in Ref. [38], by

$$\tau = \left|1 - \omega^2\frac{m_1' + m_2'}{2s} + j\omega\frac{m_1' + m_2'}{2Z_a}\left(1 - \omega^2\frac{m_1' m_2'}{s(m_1' + m_2')} + \frac{Z_a^2}{s(m_1' + m_2')}\right)\right|^{-2}, \tag{2}$$

where $\omega = 2\pi f$ is the angular frequency and

$$m_i' = m_i\left(1 - \frac{f^2}{f_{\mathrm{cr}\,i}^2}\sin^4\theta\right), i = 1, 2, \tag{3}$$

with m_i corresponding to the surface density of panel i and $f_{\mathrm{cr}} = c_0^2\sqrt{m/D}/(2\pi)$, the critical frequency of the panel, in which $D = Et^3/[12(1-\upsilon^2)]$ is the bending stiffness, with E the Young's Modulus, υ the Poisson's ratio, and t the thickness of the panel. Note that the assumption of locally reacting internal material may be affected when only gas is considered, resulting in a higher value of sound transmission loss given by the above formulas [38]. In the cases considered in the present contribution (thickness of air layer small compared to the smallest wavelength of interest), the impact associated with this internal air cavity may be relatively small.

Eq. (2) may be reformulated in the form of Eq. (1), as

$$\tau = \left|1 + \frac{Z^{\mathrm{d}}}{2Z_a}\right|^{-2}, \tag{4}$$

where the emerging impedance Z^{d} is referred to as the 'apparent impedance' of the double wall. With the purpose of extending the approach to curved double walls, this 'apparent impedance' may be rewritten as a function of the impedances of each individual panel of the system, such that

$$Z^{\mathrm{d}} = Z_1 + Z_2 + \frac{j\omega}{s}(Z_1 + Z_a)(Z_2 + Z_a). \tag{5}$$

Z_1 and Z_2 represent the impedances of the corresponding panels, and may be expressed as

$$Z_i = j\omega m_i', \quad i = 1, 2. \tag{6}$$

In Eqs. (2) and (5), $s = K/d$ is the stiffness per unit area ($\mathrm{N/m^3}$) of the air cavity, where d is the thickness of the air cavity. If the air cavity has absorbing materials, the bulk modulus K is commonly expressed as $K = \rho_0 c_0^2$. For an air cavity without absorbing material, Ref. [38] recommends $K = 4\mathrm{e}5\,\mathrm{N/m^2}$, but comparison with numerical calculations shows that 5.6e5 $\mathrm{N/m^2}$ may be better suited for the analyses conducted in the present contribution. A reason for this difference may be attributed to the locally reacting assumption of the internal material, where no sound absorbing material is introduced.

On the basis of Eq. (5), the 'apparent impedance' for a flat double wall may thus be extended to the case of a curved double wall.

2.3. 'Apparent impedance' of a curved double wall

Koval developed a theory to qualitatively describe the impedance of an 'unbounded' slightly curved panel, as [2]

$$Z^{\mathrm{c}} = \mathrm{j}\omega m\left(1 - \frac{f^2}{f_{\mathrm{cr}}^2}\sin^4\theta - \frac{{f_{\mathrm{ri}}}^2}{f^2}\right), \tag{7}$$

where $f_{\mathrm{ri}} = \sqrt{Et/m(1-\upsilon^2)}/(2\pi R)$ is the ring frequency with R the radius of curvature of the curved panel. The superscript 'c' stands here for 'curved'.

The 'apparent impedance' of a curved double wall, Z^{cd}, may thus be obtained by substituting Z_i in Eq. (5) with Z_i^{c}, such that

$$Z^{\mathrm{cd}} = Z_1^{\mathrm{c}} + Z_2^{\mathrm{c}} + \frac{\mathrm{j}\omega}{s}\left(Z_1^{\mathrm{c}} + Z_{\mathrm{a}}\right)\left(Z_2^{\mathrm{c}} + Z_{\mathrm{a}}\right). \tag{8}$$

It should be noted that s is assumed to be a constant here, and is influenced by the thickness of the air cavity. Physically, this influence of the thickness originates from the total volume of the air cavity. Thus, as long as the volume of this internal air cavity is kept constant, for minor variations of its shape, the associated stiffness per unit area from this 'air spring' may also be kept constant. As a consequence, in view of the consideration of the air cavity internal to a curved double wall, s may be obtained by averaging the thickness of that air cavity. This approximation has proved to have only marginal impact on the accuracy of the results. In particular, the assumption holds well for double walls with reasonably small curvatures, which is the case in the applications considered here. The validity of the assumption has been further verified in preliminary evaluations not reported here.

2.4. Sound transmission loss around characteristic frequencies of a slightly curved double wall

This section aims at identifying frequencies, herein referred to as the characteristic frequencies of the curved double wall, which lead to the significant dips of the transmission loss of curved double walls. For this purpose, the developments in this section focus on reconsidering the 'apparent impedance' from the transmission perspective in order to approximate the values of the characteristic frequencies of the curved double wall. For a thin flat panel, when damping is negligible, total transmission occurs at the frequency where the impedance becomes zero [30]. The same criterion may also be adopted for the curved double wall, *i.e.* that transmission loss properties collapse at frequencies where minimum impedance occurs. This reflects in the fact that the imaginary part of the impedance may become very small at these frequencies. Based on the development in this section, the two characteristic frequencies may be obtained. The approach may additionally provide an early estimate for the design of walls with specific characteristic frequencies (through the control of the ring frequency and the mass-spring-mass resonance).

The impedance for a curved double wall, expressed by Eq. (8), is detailed as

$$Z^{\mathrm{cd}} = \mathrm{j}\omega\left(m_1' + m_2'\right) + \frac{\mathrm{j}\omega}{s}\left(-\omega^2 m_1' m_2' + Z_{\mathrm{a}}^2 + \mathrm{j}\omega\left(m_1' + m_2'\right)Z_{\mathrm{a}}\right), \tag{9}$$

where in this case

$$m_i' = m_i\left(1 - \frac{f^2}{f_{\mathrm{cr}\,i}^2}\sin^4\theta - \frac{f_{\mathrm{ri}\,i}^2}{f^2}\right), \quad i = 1, 2.$$

The real and imaginary parts of the impedance may subsequently be expressed as

$$\Re\left(Z^{\mathrm{cd}}\right) = -\frac{\omega^2}{s}\left(m_1' + m_2'\right)Z_{\mathrm{a}}, \tag{10a}$$

$$\Im\left(Z^{\mathrm{cd}}\right) = \mathrm{j}\omega\left(m_1' + m_2'\right)\left(1 - \frac{\omega^2}{s}\frac{m_1' m_2'}{m_1' + m_2'} + \frac{Z_{\mathrm{a}}^2}{s\left(m_1' + m_2'\right)}\right). \tag{10b}$$

In the case where m_1 and m_2 are not too small and f is relatively large (for example, greater than 100 Hz), the condition $\omega^2 m_1 m_2 \gg Z_a^2$ will be satisfied. Consequently, in a way analogous to the simplifications in Ref. [38], the third term in the parenthesis in Eq. (10b) may be neglected.

A minimum in the transmission loss occurs when the first two terms of the imaginary part of the panel impedance cancel each other, leading to the condition

$$\omega^2 m_1' m_2' = s(m_1' + m_2'). \tag{11}$$

When $f \ll f_{cri}$, Eq. (11) may be further expressed as

$$4\pi^2 f^2 m_1 m_2 \left(1 - \frac{f_{ri1}^2}{f^2}\right)\left(1 - \frac{f_{ri2}^2}{f^2}\right) = s\left(m_1\left(1 - \frac{f_{ri1}^2}{f^2}\right) + m_2\left(1 - \frac{f_{ri2}^2}{f^2}\right)\right). \tag{12}$$

The frequency at which the sound transmission loss becomes minimum is then obtained by solving for f in Eq. (12). In general cases, the solutions for Eq. (12) are complicated functions of the masses and the corresponding ring frequencies. For a special case when two curved panels have the same ring frequency f_{ri}, the solutions for Eq. (12) are given by

$$f_1^{cd} = f_{ri}, \tag{13a}$$

$$f_2^{cd} = \sqrt{{f_{msm}^d}^2 + f_{ri}^2}, \tag{13b}$$

where f_{msm}^d is the mass-spring-mass resonance frequency of the flat double wall with parallel panels (see Fig. 1), known to be approximated as

$$f_{msm}^d = \frac{1}{2\pi}\sqrt{s\left(\frac{1}{m_1} + \frac{1}{m_2}\right)}. \tag{14}$$

f_1^{cd} and f_2^{cd} are the two characteristic frequencies of the curved double wall. It is obvious from Eq. (13) that these characteristic frequencies are actually determined by both the ring frequency of the individual curved panels and the mass-spring-mass resonance frequency of the double wall.

2.5. Metamaterial curved double wall

The locally resonant metamaterial panel consists of a host panel and periodically mounted resonators. If the distance between the resonators is much smaller than the bending wavelength in the homogenized equivalent structure, the equivalent impedance of the resonator under acoustic excitation may be expressed as [34]

$$Z_{eq}^r = j\omega m_r \frac{1}{1 - f^2/f_{res}^2}, \tag{15}$$

where m_r is the surface density of the resonator, *i.e.* the ratio of the mass of the resonator to the surface area of a lattice [27,30,34], and f_{res} is the resonance frequency of the resonator.

The effective impedance of a locally resonant metamaterial curved panel may thus be expressed as [34]

$$Z_{eff}^c = Z^c + Z_{eq}^r. \tag{16}$$

By substituting one of the individual impedances in Eq. (8) with Z_{eff}^c, an effective 'apparent impedance' of the locally resonant metamaterial curved double wall may be obtained, as

$$Z_{eff}^{cd} = Z_{eff}^c + Z^c + \frac{j\omega}{s}(Z_{eff}^c + Z_c)(Z^c + Z_c). \tag{17}$$

When both panels forming the double wall are mounted with resonators, the effective 'apparent impedance' of such metamaterial may be derived by substituting both individual impedances with the corresponding effective impedance.

The validation of the impedance approach developed herein will be provided together with the results and discussion in Sections 3 and 4.

3. Double wall with identical curved panels and associated metamaterial design

In this section, the sound transmission loss property of curved double walls is studied, for both the original and metamaterial designs. Based on these studies, a method to propose early metamaterial designs of curved double walls with good sound insulation properties is provided. In order to simplify the problem in a first step, the curved double wall studied in this section consists of two identical curved panels. This type of curved double walls is referred to herein as the identical curved double wall. Curved double walls with different curved panels will be discussed in Section 4.

A three-dimensional Finite Element model is established for the identical curved double wall and the associated metamaterial in order to simulate its transmission loss behaviour and thus validate the impedance approach, see Fig. 2. A semi-infinite curved double wall is simulated by constructing a section of the wall. Floquet periodic boundary conditions are applied for the infinite extension along the x direction, while at the bounded direction of the wall, the boundary conditions are set to be constrained. The resonators are modeled by a soft material acting as a spring and a heavy material acting as a mass (further details may be found in reference [30]). An oblique incident plane wave with an elevation angle of $\theta = \pi/3$ and an azimuthal angle of 0 degrees is defined in the incident domain, as an acoustic excitation. Non-reflecting boundary conditions, in the form of cylindrical wave radiation conditions at the corresponding boundaries, are adopted for both the incident and transmitted domains. The dimension of the mesh has been set in order to ensure the accuracy of the calculations for the shortest wavelength considered (*i.e.*, highest frequency of interest). In this paper, all the Finite Element simulations are performed using the commercial software COMSOL® [39].

In order to clarify the notations associated with a set of relevant parameters for the sample structures, and for a clear presentation of the results, an indexing system is introduced, where *e.g.*, `R1-2-40-2` refers to a curved double wall with a radius of curvature of 1 m, a thickness of the first panel of 2 mm, an air layer of 40 mm, and a thickness of the second panel of 2 mm.

In the following discussion, some selected cases are presented for the validation using the Finite Element method, and the sound transmission loss behaviour of the double wall is then investigated based on the impedance approach.

3.1. Identical curved double wall

The sound transmission loss results with the impedance approach are validated for the cases `R4-2-40-2` and `R1-2-10-2`, as shown in Fig. 3. The trends between the impedance approach and the Finite Element method are clearly the same, except for the fluctuations in the Finite Element results. These fluctuations are attributed to the eigenmodes of the structure due to the finite-sized nature of the model and the fact that only one oblique incident angle is considered in the Finite Element simulations [34]. Nevertheless, the results provided by the impedance approach, as an efficient tool, offer satisfying accuracy for the scope of the current study. In particular, the location of the characteristic frequencies, together with the associated dips in the transmission loss at these frequencies are properly captured.

Fig. 4 show the results of the sound transmission loss based on the impedance approach for curved double walls with varying parameters. As expected, the sound transmission loss exhibits dips at the two characteristic frequencies. The first dip is caused by the ring frequency effect, while the second dip is induced by the combination of the ring and mass-spring-mass resonance effects. The combination of these two dips leads to a potentially wide valley of sound transmission loss, resulting in low sound insulation performance in the associated frequency band between the characteristic frequencies. As seen in Fig. 4, the width of this frequency band may be controlled by the design parameters. This follows from Eq. (13). For a given ring frequency of the curved double wall, f_{ri}, its second characteristic frequency f_2^{cd} is fully determined by the ring

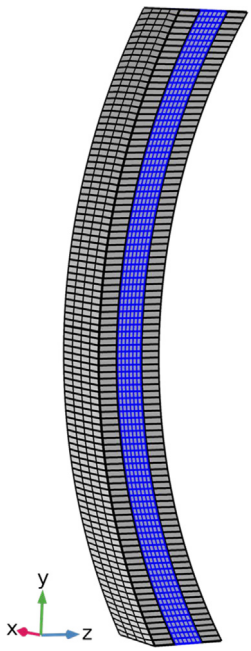

Fig. 2. A Finite Element model for the identical curved double wall.

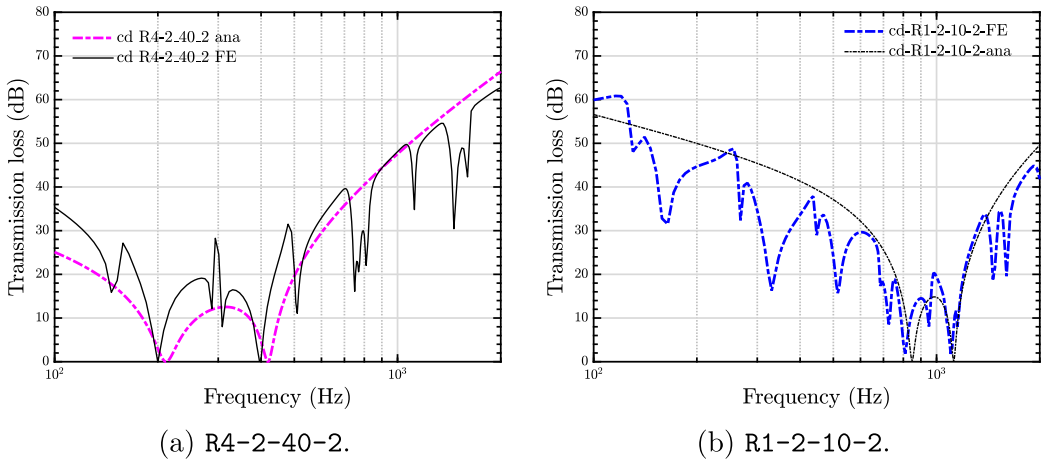

Fig. 3. Comparison of sound transmission loss between the impedance approach and the Finite Element model.

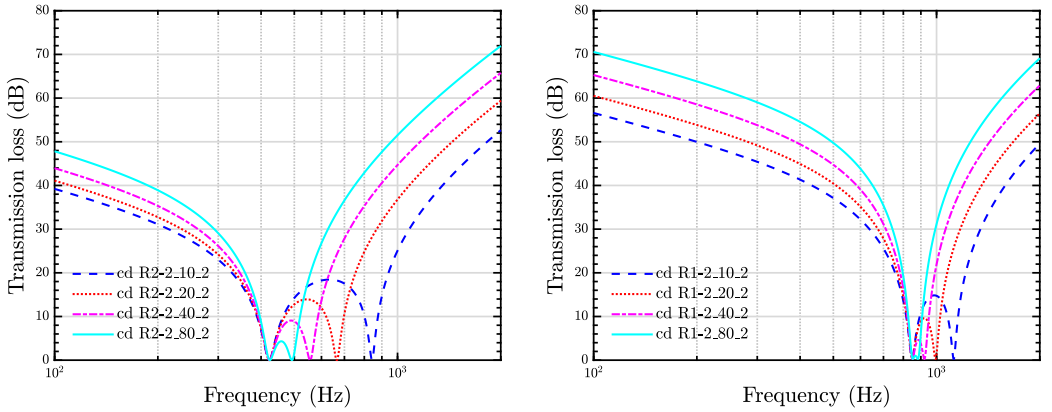

Fig. 4. Sound transmission loss of curved double walls with different parameters based on the impedance approach.

frequency itself, and the mass-spring-mass resonance frequency of the associated flat double-wall panel, $f^{\mathrm{d}}_{\mathrm{msm}}$ (see Fig. 1). This implies that the frequency band of the valley may be narrowed by controlling the second characteristic frequency to be close to the first characteristic frequency (*i.e.* the ring frequency of the outer panels in this case). Note that however close these two characteristic frequencies become, it is clear from Eq. (13) that they cannot be merged. Additionally, it is noteworthy that the closer these characteristic frequencies, the better the transmission loss properties outside of the 'valley'.

Further details are provided in Fig. 5, where the sound transmission loss of a curved double wall, a curved single-leaf panel having the same total mass, and the corresponding flat double wall having the same thickness of air cavity, are compared. As may be seen from the figure, the dip caused by the ring frequency is observed for the curved panel (blue dotted line), while the dip caused by the mass-spring-mass resonance is observed for the double wall (cyan dash-dotted line). The comparison shows that the curved double wall (red dashed line) combines the advantages of a curved panel and a flat double wall, exhibiting good sound transmission loss properties both below and above the 'valley'. The potential advantage of bringing the characteristic frequencies together is thus to concentrate the low transmission loss performance in a narrow band, which may subsequently be addressed by a localized design solution.

Before focusing on such a design, the effect of structural damping on transmission loss is introduced here. The panel `R1-2-40-2` is used for this purpose, and Fig. 6 shows the effect of structural damping η_s. For a design with a narrowed valley, introducing damping allows to improve the transmission loss in the targeted frequency range, though remaining limited by realistic values for structural damping. In order to improve the transmission loss further, a metamaterial design may be considered. Enabled by the narrowed valley emerging from the combined effect of the characteristic frequencies, local resonators may be well-suited in order to obtain a structure exhibiting improved sound insulation properties. Overcoming this valley using locally resonant metamaterial design is therefore the focus of the following section.

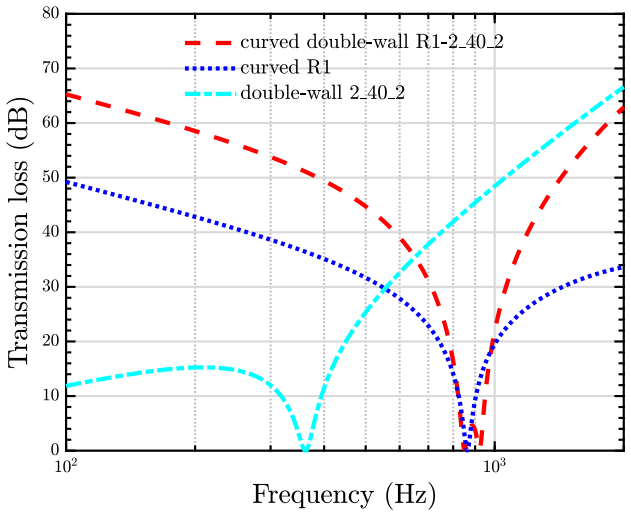

Fig. 5. Comparison of sound transmission loss for the curved panel, double wall and curved double wall.

3.2. Metamaterial design for identical curved double walls

In the metamaterial curved double wall, the mass-spring local resonators are periodically mounted on the host curved double wall. The resonance frequency of the resonator is set at the median frequency of the valley.

Two configurations for the metamaterial curved double wall are considered: *i*) Both panels of the double wall are mounted with resonators, or, *ii*) only one of the two panels of the double wall is mounted with resonators. In both cases, the total added mass is kept constant, set to be 10% of the mass of the host curved double wall. Note that the resonators are mounted on the inner surface of the panel(s) in order to avoid potential acoustic radiation [30], as shown in Fig. 7.

3.2.1. Metamaterial with resonators mounted on both panels

The sound transmission loss of the proposed metamaterial is given in Fig. 8. The host panel with the same total mass as the metamaterial is also shown for comparison. The structural damping of the host panel, for the cases presented in the following, is set to a realistic value of $\eta_s = 0.01$, unless otherwise specified. With little to no damping in the resonators, improvements appear very clearly in a narrow band associated with the combined characteristic frequencies, with however strong side effects in the form of side dips. Those side dips are then as low as the reduced transmission loss level observed in the valley area of the host panel, and within a broader overall frequency band, thus making this design practically unsuitable. Note that although the observation of these side effects is similar to the side effects observed in the ring frequency region of a

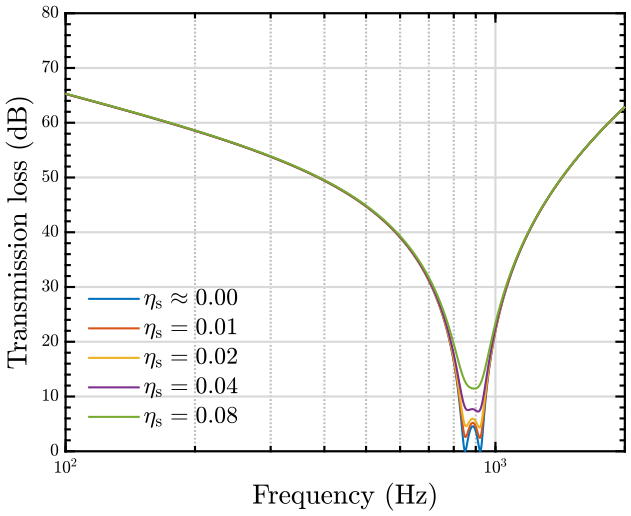

Fig. 6. The effect of structural damping η_s on sound transmission loss.

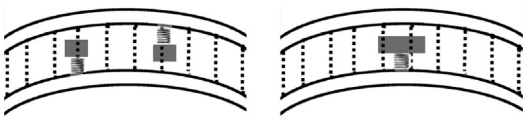

Fig. 7. Illustration of a metamaterial curved double wall with resonators mounted on both panels (left) and a single panel (right).

single curved panel, in Ref. [34], they may not be fully explained by the impedance theory in Ref. [34], as the result is here based on the 'apparent impedance' of the double wall, rather than the actual impedance of the single wall.

When damping in the resonators is increased, the side dips are mitigated, leading to an improved solution compared to the reference host panel, which is a common solution used in order to flatten the sound transmission loss curve for such metamaterial designs [40]. Next section considers the case when the resonators are mounted on one of the two panels only.

3.2.2. Metamaterial with resonators mounted on a single panel

Fig. 9 shows the sound transmission loss when the resonators are mounted on one panel only. Such metamaterial solution for double-wall systems may also be found in Refs. [35,33]. Note that the resonant mass added to one panel is doubled compared to the former case since the total mass of the structure is unchanged. It may be expected that these two configurations of the resonators lead to different dynamic behaviours of the resonator, thus causing changes in the 'apparent impedance' of the corresponding metamaterial curved double wall. For a set level of damping in the resonators, the results are much improved compared to the case where resonators are mounted on both panels. This improvement, and associated change of dynamic behaviour when the resonators are mounted on a single or both panels, (Figs. 8 and 9), lies in the fact that there is a difference of a term $\left(\mathrm{j}\frac{\omega}{s}Z_{\mathrm{eq}}^2\right)$ in the apparent impedance between the two cases, where Z_{eq} is the equivalent impedance of one of the two resonators on the panels (see Eq. (17)). Physically, this indicates that the effective impedance of the resonators, when mounted on one or two panels, varies with different rates as a function of frequency. Although the sound transmission loss at the characteristic frequencies is not as drastically improved, the change in the resonator performance compared to the first case leads to the interesting observation that the side dips are mitigated such that the overall performance of the panel is improved. For example, a minimum improvement of about 5 dB is observed for the side dips of the chosen cases, *i.e.* $\eta_{\mathrm{r}} = 0.01$ (cyan solid line in Figs. 8 and 9) and $\eta_{\mathrm{r}} = 0.08$ (red dash-dot line in Figs. 8 and 9). Interestingly, due to the fact that the peak appearing at the resonance frequency of the resonator is progressively converted into a dip when the damping is increased at realistic values, a trade-off against the improvement of the side dips is to be found. This trade-off is further illustrated with a parametric study with respect to the damping of the resonator, as shown in Fig. 10. The optimal configuration may be found when the side dips and the transmission loss at the resonance frequency of the resonators reach similar levels. In the present situation, as illustrated in Fig. 10 both using the impedance approach and the Finite Element model, this configuration is met for $\eta_{\mathrm{r}} \approx 0.08$. This configuration leads to a transmission loss being higher than 20 dB in the critical frequency band associated with the characteristic frequencies.

Furthermore, Fig. 11 show the effect of taking into account the structural damping of the panels while the damping of the resonators is kept to the previously found value of 0.08, both for the impedance approach and the Finite Element validation. The structural damping further flattens the transmission loss thus slightly improving the overall performance.

Finally, in order to provide an engineering perspective, a comparison of the transmission loss in 1/3 octave bands is plotted in Figs. 12 and 13, based on the Finite Element calculations. The host panel is taken as a reference in both plots (dashed

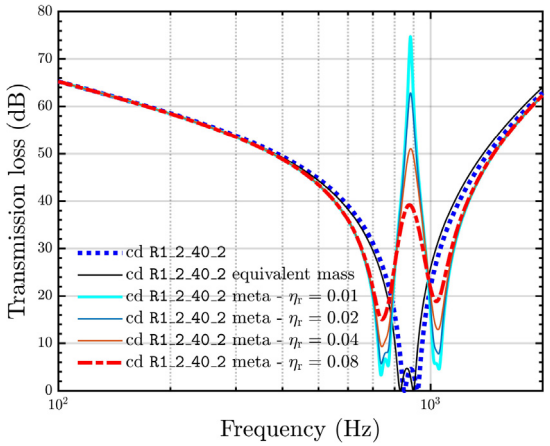

Fig. 8. Sound transmission loss of the metamaterial curved double wall with the resonators mounted on both panels, with damping η_{r} in the resonators.

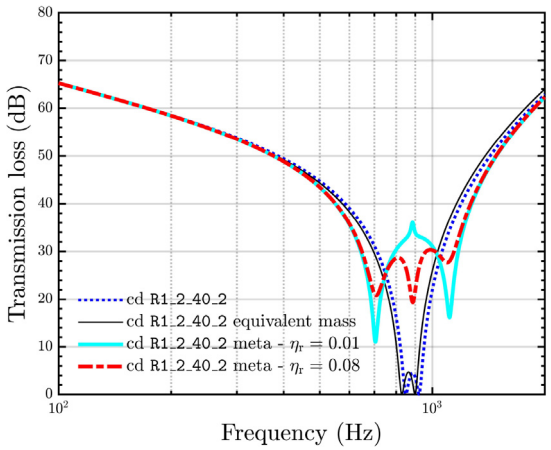

Fig. 9. Sound transmission loss of metamaterial curved double wall, with the resonators mounted on one of the two panels out of curved double wall, with $\eta_r = 0.01$ for the cyan solid line and $\eta_r = 0.08$ for the red dash-dot line. (For interpretation of the references to color in this figure legend, the reader is referred to the web version of this article.)

blue curves). Fig. 12 shows that a curved double wall has the advantage of exhibiting good sound insulation properties both below and above the characteristic frequencies. Further using a metamaterial design in order to address the bad performance in this narrow frequency band allows to ensure improved sound insulation properties over the entire frequency range of interest (see Fig. 13).

4. Double wall with different curved panels and associated metamaterial design

In practical designs, nonidentical curved double walls, consisting of two different curved panels, are more common than identical curved double walls. For nonidentical curved double walls, the differences between the curved panels may be sought in terms of material and geometric properties. An example of such nonidentical curved double wall is the side wall of an aircraft fuselage, which consists of a skin panel and a trim panel. Taking the side wall as an example, a Finite Element model is constructed in order to simulate the transmission loss behaviour of such structures, as shown in Fig. 14. Note that, although in most cases the difference between the skin panel and the trim panel may result in different ring frequencies, these may be tuned to the same frequency by design. These two cases are investigated in the following discussion, using both the impedance approach and Finite Element simulations. The material and geometric properties used for the skin and the trim panels are shown in Table 1.

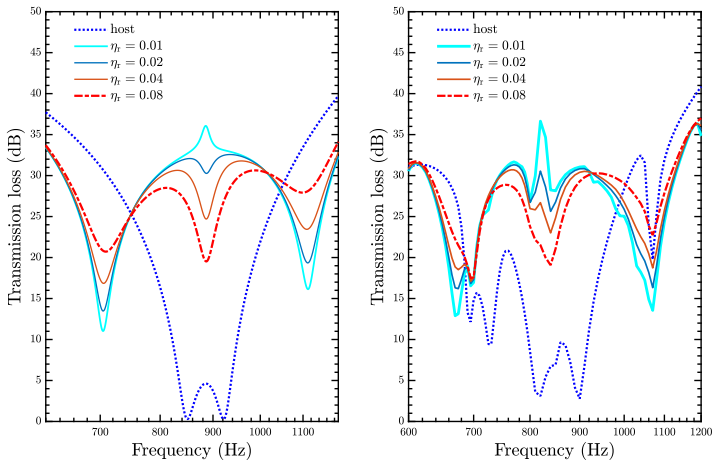

(a) Impedance approach. (b) Finite Element models.

Fig. 10. A detailed parametric study of the damping effect on sound transmission loss behaviour.

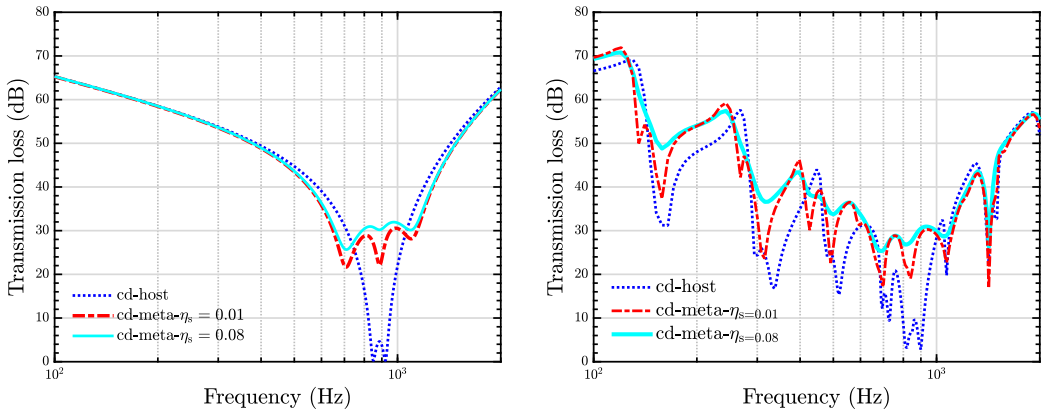

(a) Impedance approach. (b) Finite Element model.

Fig. 11. Effect of structural damping on the sound transmission loss behaviour of the metamaterial curved double wall, with damping of the resonators $\eta_r = 0.08$.

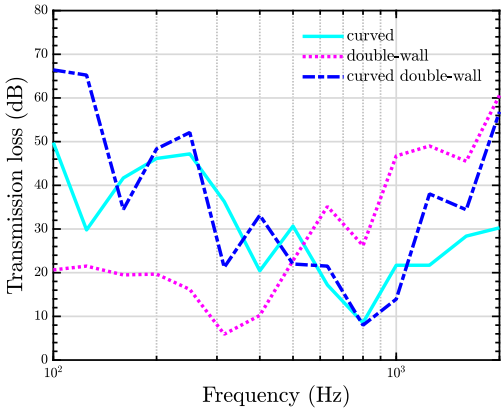

Fig. 12. Sound transmission loss of curved panel, double wall and curved double wall in 1/3 octave bands.

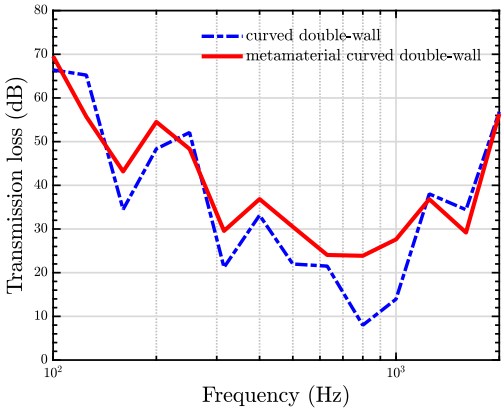

Fig. 13. Sound transmission loss of curved double wall and the metamaterial in 1/3 octave bands.

4.1. Nonidentical curved double wall with distinct ring frequencies

First, the nonidentical curved double wall is such that it has two distinct ring frequencies (skin and trim panel 1). The resulting sound transmission loss is shown in Fig. 15. As may be seen, there are two dips in the sound transmission loss curve (blue dotted line), associated with the solutions of Eq. (12) for general cases.

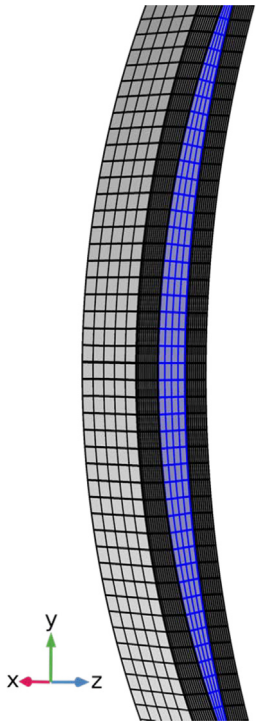

Fig. 14. A Finite Element model for the nonidentical curved double wall.

In order to overcome these two dips, the two curved panels are respectively equipped with resonators whose resonance frequencies are set to match the frequencies of the dips. The added mass is maintained at 10% of the total mass of the host structure and is equally distributed on the two curved panels. As may be seen in Fig. 15, both the impedance approach and the Finite element results show that these resonators allow to overcome these dips (red solid line), given here $\eta_s = 0.01$, and $\eta_r = 0.08$.

4.2. Nonidentical curved double wall with the same ring frequency

In the second case, the skin panel and the trim panel 2 are used to form the curved double wall, such that the curved panels constituting the double wall have the same ring frequency.

From the results of the sound transmission loss in Fig. 16, similar acoustic behavior to the identical curved double walls previously discussed in Section 3.2.2 may be observed, indicating that such a configuration may respond well to a similar metamaterial design. Indeed, an improvement of more than 15 dB may be observed at the dip associated with the characteristic frequencies of the curved double wall by using suitably damped resonators, both for the impedance approach (red solid line in Fig. 16(a)) and the Finite Element model (red solid line in Fig. 16(b)). The sound transmission loss results in 1/3 octave bands, using identical damped resonators attached to one of the panels, are shown in Fig. 17. Similar conclusions may be drawn from this plot, *i.e.* an overall improved performance due to the sharp improvements of the transmission loss in the region of the characteristic frequencies (15 to 20 dB in the present case).

5. Conclusions

Locally resonant metamaterial curved double walls are proposed and their sound insulation properties investigated. In particular, a method for designing such panels is proposed in order to improve their overall sound insulation in a broad range

Table 1
Material properties of the skin panel and the trim panel.

	E (Pa)	υ (–)	ρ(kg/m^3)	R (m)	f_{ring} (Hz)
Skin	6.9e10	0.3	2700	1	843
Trim 1	3e9	0.4	1400	1.4	182
Trim 2	5e10	0.4	1000	1.445	843

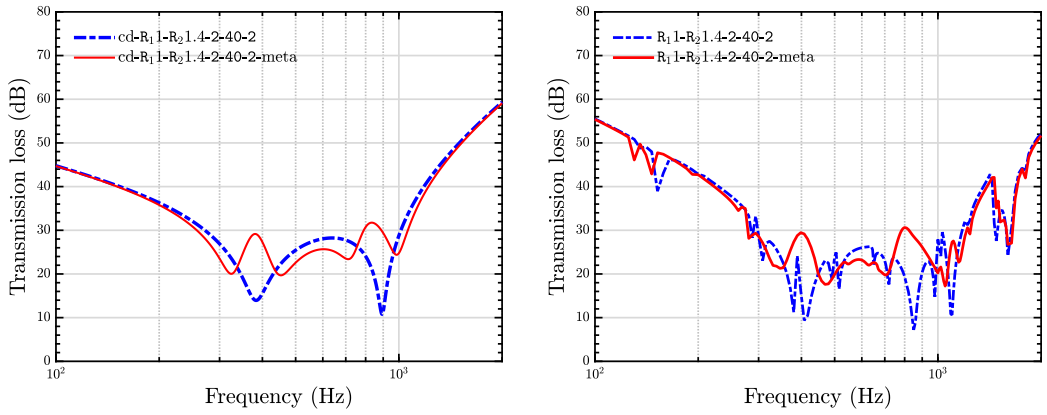

(a) Impedance approach. (b) Finite Element method.

Fig. 15. Sound transmission loss of a nonidentical curved double wall with distinct ring frequencies.

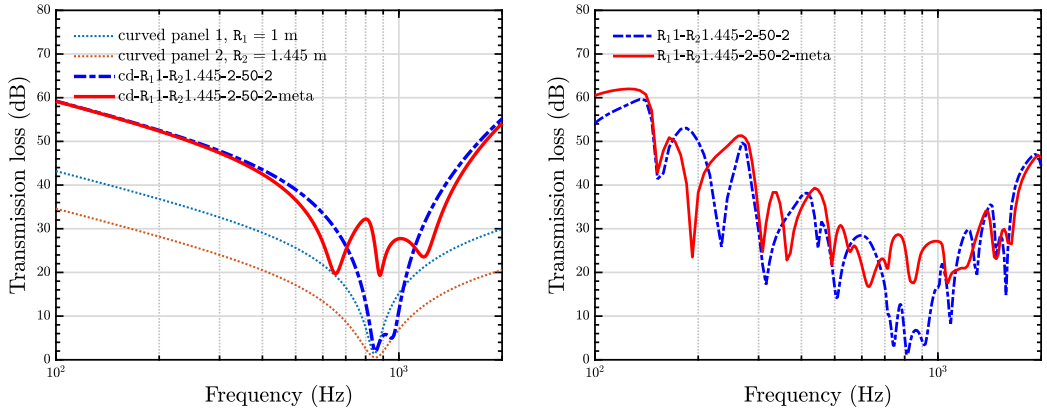

(a) Impedance approach. (b) Finite Element method.

Fig. 16. Sound transmission loss of a nonidentical curved double wall with the same ring frequency.

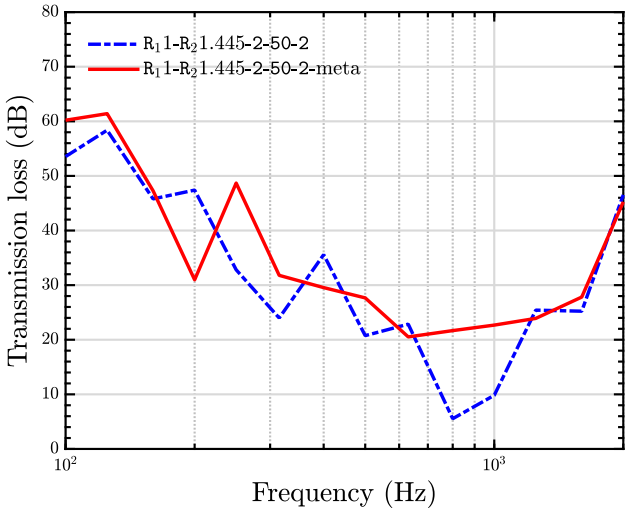

Fig. 17. Sound transmission loss of the nonidentical curved double wall and the metamaterial provided in 1/3 octave bands.

around characteristic frequencies in the low frequency region. In order to conduct the analyses associated with the development of this design methodology, an effective impedance approach, referred to as an 'apparent impedance' approach, is proposed for the estimation of the sound transmission loss of the curved double wall and its metamaterial description. This impedance approach is validated against a Finite Element model, showing a good ability to capture the main trends of the transmission, in particular accurately locating the effects associated with the characteristic frequencies of the curved double wall and the resonance of the resonators. The impedance approach thus proves to be a valuable tool for conducting effective pre-studies before more expensive simulations/experiments are undertaken.

In the proposed design methodology, the two characteristic frequencies, associated with the ring frequency and the mass-spring-mass resonance frequency of the curved double wall, are designed to be very close to each other, such that the curved double wall combines the advantages of a curved panel and a double-wall structure: good sound insulation properties associated with the curved panels below the ring frequency, and good acoustic properties associated with the double walls above the mass-spring-mass resonance. Then, by incorporating close-to-optimally damped resonators on one of the panels of the curved double wall, the transmission drop in the region of the characteristic frequencies of the host structure may be effectively addressed. As illustrated with the extension to nonidentical curved double walls (*i.e.* where the outer panels have both different geometric and material properties), the resulting design methodology to improve noise insulation properties offers a valuable degree of robustness. The design results presented in this contribution are considered to be further validated with experimental studies.

CRediT authorship contribution statement

Zibo Liu: Conceptualization, Methodology, Software, Investigation, Data curation, Writing - original draft, Writing - review & editing. **Romain Rumpler:** Conceptualization, Methodology, Software, Investigation, Data curation, Writing - review & editing, Supervision. **Leping Feng:** Conceptualization, Methodology, Investigation, Data curation, Supervision.

Declaration of Competing Interest

The authors declare that they have no known competing financial interests or personal relationships that could have appeared to influence the work reported in this paper.

Acknowledgment

The authors are grateful for the financial support provided by the KTH-CSC Programme (No. 201403170345). The Swedish Research Council (VR Grant 2015-04925) and the Centre for ECO2 Vehicle Design (Sweden's Innovation Agency VINNOVA, Grant No. 2016-05195) are gratefully acknowledged for their financial support of the authors.

References

[1] P. Smith Jr, Sound transmission through thin cylindrical shells, The Journal of the Acoustical Society of America 29 (6) (1957) 721–729.
[2] L.R. Koval, On sound transmission into a thin cylindrical shell under "flight conditions", Journal of Sound and Vibration 48 (2) (1976) 265–275.
[3] L.R. Koval, Effect of air flow, panel curvature, and internal pressurization on field-incidence transmission loss, The Journal of the Acoustical Society of America 59 (6) (1976) 1379–1385.
[4] L.R. Koval, On sound transmission into an orthotropic shell, Journal of Sound and Vibration 63 (1) (1979) 51–59.
[5] L.R. Koval, Sound transmission into a laminated composite cylindrical shell, Journal of Sound and Vibration 71 (4) (1980) 523–530.
[6] A. Blaise, C. Lesueur, M. Gotteland, M. Barbe, On sound transmission into an orthotropic infinite shell: comparison with koval's results and understanding of phenomena, Journal of Sound and Vibration 150 (2) (1991) 233–243.
[7] S. Ghinet, N. Atalla, H. Osman, The transmission loss of curved laminates and sandwich composite panels, The Journal of the Acoustical Society of America 118 (2) (2005) 774–790.
[8] B. Liu, L. Feng, A. Nilsson, Sound transmission through curved aircraft panels with stringer and ring frame attachments, Journal of Sound and Vibration 300 (3–5) (2007) 949–973.
[9] B. Liu, L. Feng, A. Nilsson, Influence of overpressure on sound transmission through curved panels, Journal of Sound and Vibration 302 (4–5) (2007) 760–776.
[10] F. Errico, F. Franco, S. De Rosa, G. Petrone, M. Ichchou, Aeroelastic effects on wave propagation and sound transmission of plates and shells, AIAA Journal (2019) 1–7.
[11] F. Errico, G. Tufano, O. Robin, N. Guenfoud, M. Ichchou, N. Atalla, Simulating the sound transmission loss of complex curved panels with attached noise control materials using periodic cell wavemodes, Applied Acoustics 156 (2019) 21–28.
[12] C. Droz, O. Robin, M. Ichchou, N. Atalla, Improving sound transmission loss at ring frequency of a curved panel using tunable 3d-printed small-scale resonators, The Journal of the Acoustical Society of America 145 (1) (2019) EL72–EL78..
[13] A. London, Transmission of reverberant sound through double walls, The Journal of the Acoustical Society of America 22 (2) (1950) 270–279.
[14] F. Sgard, N. Atalla, J. Nicolas, A numerical model for the low frequency diffuse field sound transmission loss of double-wall sound barriers with elastic porous linings, The Journal of the Acoustical Society of America 108 (6) (2000) 2865–2872.
[15] J. Wang, T. Lu, J. Woodhouse, R. Langley, J. Evans, Sound transmission through lightweight double-leaf partitions: theoretical modelling, Journal of Sound and Vibration 286 (4–5) (2005) 817–847.
[16] S.J. Pietrzko, Q. Mao, New results in active and passive control of sound transmission through double wall structures, Aerospace Science and Technology 12 (1) (2008) 42–53.
[17] J. Zhou, A. Bhaskar, X. Zhang, Sound transmission through a double-panel construction lined with poroelastic material in the presence of mean flow, Journal of Sound and Vibration 332 (16) (2013) 3724–3734.
[18] W. Larbi, J. Deü, R. Ohayon, Vibroacoustic analysis of double-wall sandwich panels with viscoelastic core, Computers & Structures 174 (2016) 92–103.

[19] J. Li, S. Li, Sound transmission through metamaterial-based double-panel structures with poroelastic cores, Acta Acustica united with Acustica 103 (5) (2017) 869–884.
[20] C. Soussi, W. Larbi, J.-F. Deü, Experimental and numerical analysis of sound transmission loss through double glazing windows, in: International Conference on Acoustics and Vibration, Springer, 2018, pp. 195–203..
[21] J.-H. Lee, J. Kim, Analysis and measurement of sound transmission through a double-walled cylindrical shell, Journal of Sound and Vibration 251 (4) (2002) 631–649.
[22] J. Zhou, A. Bhaskar, X. Zhang, The effect of external mean flow on sound transmission through double-walled cylindrical shells lined with poroelastic material, Journal of Sound and Vibration 333 (7) (2014) 1972–1990.
[23] Y. Liu, C. He, On sound transmission through double-walled cylindrical shells lined with poroelastic material: comparison with zhous results and further effect of external mean flow, Journal of Sound and Vibration 358 (2015) 192–198.
[24] M. Badreddine Assouar, M. Senesi, M. Oudich, M. Ruzzene, Z. Hou, Broadband plate-type acoustic metamaterial for low-frequency sound attenuation, Applied Physics Letters 101 (17) (2012) 173505..
[25] Y. Xiao, J. Wen, X. Wen, Sound transmission loss of metamaterial-based thin plates with multiple subwavelength arrays of attached resonators, Journal of Sound and Vibration 331 (25) (2012) 5408–5423.
[26] M. Oudich, X. Zhou, M. Badreddine Assouar, General analytical approach for sound transmission loss analysis through a thick metamaterial plate, Journal of Applied Physics 116 (19) (2014) 193509..
[27] Y. Song, L. Feng, J. Wen, D. Yu, X. Wen, Reduction of the sound transmission of a periodic sandwich plate using the stop band concept, Composite Structures 128 (2015) 428–436.
[28] H. Zhang, J. Wen, Y. Xiao, G. Wang, X. Wen, Sound transmission loss of metamaterial thin plates with periodic subwavelength arrays of shunted piezoelectric patches, Journal of Sound and Vibration 343 (2015) 104–120.
[29] T. Wang, M. Sheng, Q. Qin, Sound transmission loss through metamaterial plate with lateral local resonators in the presence of external mean flow, The Journal of the Acoustical Society of America 141 (2) (2017) 1161–1169.
[30] Z. Liu, R. Rumpler, L. Feng, Broadband locally resonant metamaterial sandwich plate for improved noise insulation in the coincidence region, Composite Structures 200 (2018) 165–172.
[31] Y. Song, L. Feng, Z. Liu, J. Wen, D. Yu, Suppression of the vibration and sound radiation of a sandwich plate via periodic design, International Journal of Mechanical Sciences 150 (2019) 744–754.
[32] F. Errico, M. Ichchou, S. De Rosa, F. Franco, O. Bareille, Investigations about periodic design for broadband increased sound transmission loss of sandwich panels using 3d-printed models, Mechanical Systems and Signal Processing 136 (2020), 106432.
[33] N. de Melo Filho, C. Claeys, E. Deckers, W. Desmet, Metamaterial foam core sandwich panel designed to attenuate the mass-spring-mass resonance sound transmission loss dip, Mechanical Systems and Signal Processing 139 (2020), 106624.
[34] Z. Liu, R. Rumpler, L. Feng, Investigation of the sound transmission through a locally resonant metamaterial cylindrical shell in the ring frequency region, Journal of Applied Physics 125 (11) (2019), 115105.
[35] N. de Melo Filho, L. Van Belle, C. Claeys, E. Deckers, W. Desmet, Dynamic mass based sound transmission loss prediction of vibro-acoustic metamaterial double panels applied to the mass-air-mass resonance, Journal of Sound and Vibration 442 (2019) 28–44.
[36] Y. Xiao, J. Wen, X. Wen, Flexural wave band gaps in locally resonant thin plates with periodically attached spring–mass resonators, Journal of Physics D: Applied Physics 45 (19) (2012), 195401.
[37] A. Nateghi, L. Sangiuliano, C. Claeys, E. Deckers, B. Pluymers, W. Desmet, Design and experimental validation of a metamaterial solution for improved noise and vibration behavior of pipes, Journal of Sound and Vibration 455 (2019) 96–117.
[38] M. Heckl, The tenth sir richard fairey memorial lecture: sound transmission in buildings, Journal of Sound and Vibration 77 (2) (1981) 165–189.
[39] COMSOL, Introduction to COMSOL Multiphysics, 1998– 2017. URLhttps://cdn.comsol.com/documentation/5.3.0.316/IntroductionToCOMSOLMultiphysics.pdf..
[40] L. Van Belle, Vibro-acoustic performance of locally resonant metamaterials with damping (2019). URL $$Uhttps://lirias.kuleuven.be/retrieve/539861$$DPhDThesis_LucasVanBelle_2019.pdf [freely available]..